

The onset of chaos in the wake of an oscillating cylinder: Experiment and the dynamics of the circle map

D J OLINGER¹, A B CHHABRA² and K R SREENIVASAN³

¹Mechanical Engineering, Worcester Polytechnic Institute, Worcester, MA 01609, USA

²Chemical Bank, New York, NY 10021, USA

³Mason Laboratory, Yale University, New Haven, CT 06520, USA

Abstract. This paper deals with a comparison between experimental observations in a low-Reynolds-number wake behind an oscillating cylinder and the universal properties of a sine circle map. When the limit cycle due to the natural vortex shedding in the wake is modulated at a second frequency by oscillating the cylinder transversely, one obtains in phase space a flow on a two torus. The nonlinear interaction between the two oscillators results in Arnol'd tongues due to phase locking, the devil's staircase along the critical line, and a transition from order to chaos *via* the quasiperiodic route. The sine circle map describes these features adequately. A comparison between the experiment and the theory is made in terms of multifractal formalism and trajectory scaling function.

Keywords. Chaos; universality; circle maps; wakes.

PACS Nos 47.52; 47.27

1. Introduction

One of the major hopes in modern nonlinear dynamics is that it might shed some light on the long-standing problem of fluid turbulence. A specific aspect concerns the relevance of dissipative chaos to understanding facets of the onset of turbulence. There now exist sufficiently detailed predictions on the occurrence of chaos for some simple dynamical systems. There also exist several experiments on fluid flows purporting to make quantitative comparisons with theoretical scenarios of dissipative chaos. The agreement has often been astonishingly good. A convenient collection of seminal papers on this subject can be found in Ref. [1].

For a first sight, it appears surprising that there should be this precise correspondence between some one-dimensional maps (or similarly simple dynamical systems) and fluid systems governed by partial differential equations. This deep and fascinating fact is attributed to two important properties of dissipative systems: (a) Dissipation stabilizes orbital instability and contracts the phase space, and allows some high-dimensional systems under certain circumstances to assume low-dimensional characteristics; (b) low-dimensional systems enjoy “universal” properties—that is, many measurable properties of a system can be quantitatively determined, independent of its specific details, by certain qualitative attributes. While it is true that not every system can be fitted into this scenario, its occurrence—even if special—is worth a serious study.

In this paper, we are concerned with the demonstration that the universal properties of the quasiperiodic route to chaos in the sine circle map ([2], [3], [4]) is an appropriate framework for describing the low-Reynolds-number behavior of the wake behind an oscillating cylinder. Previous experimental studies of this nature in this particular flow can be found in Refs. [5] and [6], and similar studies in other fluid flows in Refs. [7], [8], [9], and [10]. This paper is in some respects a synopsis of results obtained a few years ago [11], but it also presents some that have not been published before.

2. The flow

We study the wake of an oscillating circular cylinder of diameter 0.5 mm, housed in a low-noise suction-type wind tunnel, and oscillated electromagnetically in the direction transverse to that of upstream fluid velocity. In practice, the oscillating cylinder is a stainless steel string of uniform diameter stretched taut, through the wind tunnel walls, over a distance that is four times the tunnel span. The active length/diameter ratio of the cylinder is about 300. The Reynolds number based on the cylinder diameter and the velocity of the oncoming air flow is 55. We place a velocity sensor at a distance of 15 diameters behind the cylinder, half a diameter off the geometric axis of the stationary wake. The velocity sensor is a standard hotwire of 5 μm diameter and 0.6 mm length, operated on a constant temperature anemometer. The sensor measures the streamwise component of fluid velocity. For more details of the experimental arrangement, instrumentation and data processing, please see Ref. [11].

The regular ‘shedding’ of vortices at Reynolds numbers above about 40 imparts to the wake a periodic motion of frequency f_o , say. The frequency f_o is a known function of the Reynolds number [12]. The transverse oscillation at the controlled frequency f_e imposes a second frequency on the wake. The amplitude of oscillation of the cylinder can be thought of as a coupling parameter between vortex shedding and cylinder oscillation. This nonlinear coupling “shifts” the shedding frequency to some neighboring value, say f'_o , which depends on the ratio $\Omega = f_e/f_o$ and the magnitude of the nonlinear coupling between the two oscillators. In the jargon of quasiperiodic dynamical systems, the parameter $\Omega = f_e/f_o$ is called the bare winding number, and the ratio $\omega = f_e/f'_o$ is called the dressed winding number.

3. The circle map

Systems with two independent frequencies f_o and f_e define a torus in the phase space. As the system evolves, the phase space trajectory hits a Poincaré section at some discrete iterates along a circle. The angular position of the iterates is the variable of dynamical interest. A paradigm situation is given by the sine circle map

$$\theta_{n+1} = \theta_n + \Omega - \frac{K}{2\pi} \sin(2\pi\theta_n), \quad (1)$$

where θ_n is the angular coordinate of the n^{th} iterate, Ω is the bare winding number and $K > 0$ is the nonlinear coupling parameter. The map is utilized by setting $0 < \Omega < 1$ and

obtaining the iterates of θ . The dressed winding number is defined as $\omega = \lim_{n \rightarrow \infty} [(\theta_n - \theta_0)/n]$.

The experimental situation is qualitatively similar to that encountered in circle maps; following the spirit of universality mentioned above, it appears reasonable to explore the analogies quantitatively. For this purpose, we should recall a few key results about the circle map, known from the theoretical analysis of Refs. [2]–[4]:

- For low forcing amplitudes, equation (1) exhibits Arnol'd tongues (regions of mode locking) in which the frequency f_o shifts so that the dressed winding number is fixed as a rational over some finite range of f_e .
- In other case where the dressed winding number is irrational, the motion is quasiperiodic.
- As the nonlinear coupling parameter K increases, the Arnol'd tongues widen; they overlap at some critical line corresponding to the critical value of K . This critical line corresponds to the breakdown of the two torus and the onset of chaos.
- Along the critical line, the system exhibits the devil's staircase structure.
- A special case of interest is the locus of the position in the $K - \Omega$ space where the dressed winding number is the inverse of the golden mean. (Loosely speaking, golden mean $\equiv (\sqrt{5} - 1)/2$ is the "most" irrational number, or least well represented by a rational approximation, because its continued fraction representation contains only the numeral one.) At the critical point on this line, where $\omega = \sigma_g$, the latter being the inverse of the golden mean, the system is least influenced by mode-locking and is quasiperiodic. The properties of the system at this critical point are universal.
- At the critical point, the power spectrum of the angular variable has a certain well-quantified self-similar structure [2].
- A description of this behavior requires modern dynamical systems theory including multifractals [13] and scaling functions [2].

4. Devil's staircase and power spectral density

In Refs. [5] and [11], it was shown that most of these properties were exhibited by the wake of the oscillating cylinder. As a quick recapitulation, we show in figure 1 the devil's staircase structure along the critical line. The small circles mark the extremes of a few principal Arnol'd tongues corresponding to the rational values of the dressed winding number marked on the figure. These are to be compared with the horizontal bars representing the theoretical results for the circle map. The comparison is good on the whole. Many other tongues were mapped out experimentally but are not given on the figure. A few narrower tongues near the rational numbers $4/15$ to $5/16$ are displayed in the inset. The general pattern is the same as that of the circle map, although some visible differences occur.

As a second example of the correspondence between the wake and the circle map, we show in figure 2 the scaled power spectral density of the velocity signal obtained close to the critical point. As known for the circle map dynamics, we have (nearly) equal-amplitude spectral peaks, marked 1, at powers of σ_g up to the fifth. For higher powers, the flow system does not respond like the circle map, yet the appearance of these equally-spaced peaks is quite encouraging. Furthermore, between any two of the four right-most

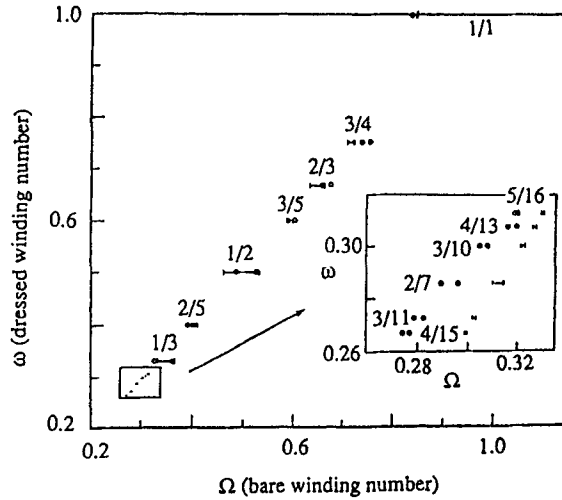


Figure 1. The devil's staircase showing mode-lockings along an experimentally determined critical line (circles). The general pattern is similar to that of the circle map (bars). The inset expands the small rectangle to the lower left.

primary spectral peaks, there are families of peaks marked 2, 3, 4 and 5, which—where they exist—appear at the right place according to the circle map theory. More delicate fine structure in the circle map is not replicated by the fluid system. It is difficult to say if these differences are real or if the fluid system is not exactly at the critical point as the theory demands. Locating the critical point is quite delicate, and the results are conspicuously sensitive to the precise location in its neighborhood [11]. Independent of this uncertainty, it is fair to say that the wake behaves, at least grossly, much like a circle map. This then suggests that the underlying dynamics of this fluid system may live on a low-dimensional attractor whose Poincaré section closely resembles that generated by the circle map. This expectation is explored in greater detail below.

5. Multifractal analysis

To construct the experimental Poincaré section at the critical point in phase space, the continuous hotwire velocity time trace $u(t)$ is sampled discretely at a time period τ equal to the period of excitation, yielding $P_n = u(t + n * \tau)$, $n = 0, 1, 2, 3, \dots$. This procedure can lead to some problems if there is a drift in the bare or dressed winding numbers. A better procedure is to select points in the continuous time trace which have zero time derivative. In either case, the P_n are embedded in the three-dimensional phase space (P_n, P_{n+1}, P_{n+2}) , three being the lowest dimension in which the P_n are non-interacting. A two-dimensional projection of the three-dimensional Poincaré section is shown in figure 3. The attractor lies essentially on a one-dimensional subspace and is perceptibly inhomogeneous. (Other projections described in Ref. [11] confirm this conclusion.)

We first turn to a suitable statistical characterization of the attractor. From the theory of circle maps, one knows that the attractor generated from the sine circle map has a

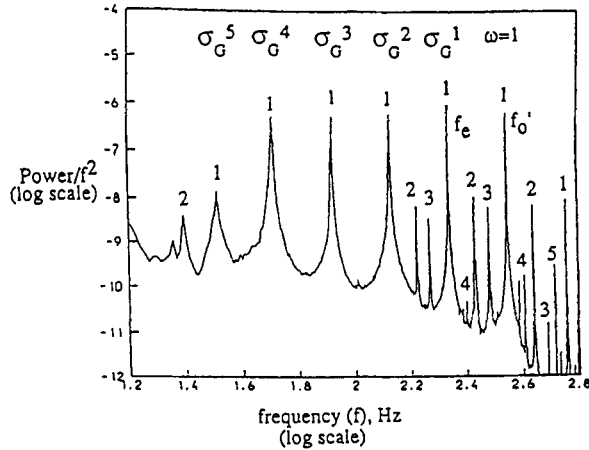


Figure 2. The scaled power spectral density for the velocity signal measured in the wake of the oscillating cylinder. The dressed winding number is estimated to be within 0.1 % of σ_g . The structure is quantitatively similar to that of the circle map.

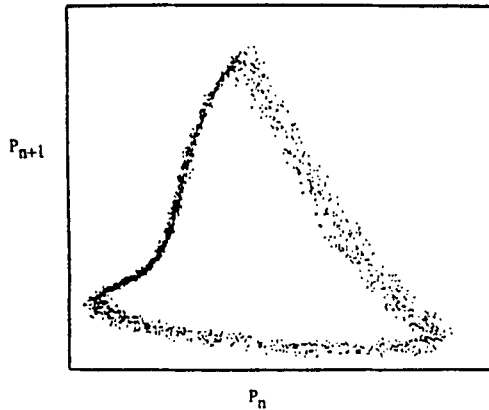


Figure 3. Two-dimensional projection of the experimental Poincaré section at the critical golden mean point, obtained by embedding the velocity signal in three dimensions as described in the text.

particular self-similar structure that can be quantified *via* the multifractal formalism. Exploitation of this self-similar structure for making predictions about the dynamics of the system is the goal of the multifractal formalism. To this end, one can construct a measure on this attractor by subdividing it into boxes of equal size and computing the density of points in each of these boxes. This gives one a measure of how often certain regions of the attractor are visited in comparison with others. One defines a singularity strength [13] by

$$\pi_i \sim L^{\alpha_i}, \tag{2}$$

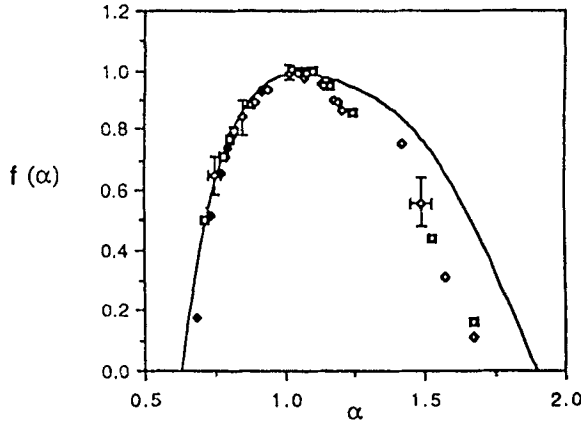


Figure 4. The $f(\alpha)$ curve obtained from analyzing the measure on the Poincaré section. The solid line is the theoretical curve for the sine circle map at the golden mean critical point. Typical error bars are shown.

where π_i is the relative density of points in the i^{th} box of size L . The box size L is restricted to the scaling bounded by some inner and outer cut-off scales. Within the scaling range, one can define $f(\alpha)$ as the dimension of the set of points possessing singularity strength α by the equation

$$N(\alpha) \sim L^{-f(\alpha)}, \tag{3}$$

where $N(\alpha)$ is the number of boxes of size L possessing singularity strength α . The $f(\alpha)$ formalism entails viewing the attractor as the union of several interwoven fractal sets each having a measure of a different singularity strength. (In equations (2) and (3), the symbol \sim subsumes all the prefactors needed to render them dimensionally homogeneous.)

A summary of these multifractal results is given in figure 4 which shows a comparison between the measured $f(\alpha)$ curve at the experimentally determined critical point and that for the sine circle map. Space limitations preclude a description here of how the curve was obtained from experimental data. This information can be found in Ref. [11]. On the left part of the figure representing the scaling of high probability regions on the attractor, the data agree well with the circle map predictions. The right half of the $f(\alpha)$ curve represents the scaling of the low-probability events on the attractor and is usually unreliable in experiment because of the strong influence of noise (even if small). It is thus unclear at present whether the discrepancy on the right part represents a true departure from the universal scaling or is an experimental artifact.

We have discussed this issue in more detail in Refs. [11] and [14] where we have concluded that the correspondence between the circle map and the flow is indeed real.

6. The trajectory scaling function

One would like to push further the correspondence between the flow and the circle map. One powerful way of describing the dynamics of a system is the so-called Feigenbaum

scaling function [15], [16]. This object contains microscopic information about a deterministic dynamical system and its scaling properties. At the onset of chaos, the attractor can be regarded as constructed by an underlying multiplicative process that successively refines it, in such a way that it possesses scaling properties at finer and finer scales. The scaling function gives a compact description of the refinement basic to the fractal structure of the attractor. The underlying multiplicative process can be mapped on to a subdividing tree structure where, on the average, each branch divides into 2 subbranches at each successive level of refinement. The iterates of the dynamical system become branches of the tree, and intervals are formed by joining nearest neighbor branches.

At the critical golden mean winding number, the attractor can be thought to have been generated by successive refinements of a measure created from superstable periodic orbits whose winding numbers are successive Fibonacci approximations to the golden mean. The Fibonacci sequence is given by the relation $F_{i+2} = F_i + F_{i+1}$ with $F_0 = 0$ and $F_1 = 1$. It is easily verified that the ratio $p/q = F_i/F_{i+1}$ approaches σ_g for large enough i . Since the intervals at each level are formed by joining nearest neighbor points, a measure is constructed to give equal weight to each such interval. The scaling function, which describes the contraction factors of each interval along each branch as the tree subdivides, is defined as

$$\sigma_\ell(\epsilon_{n+1}, \dots, \epsilon_o) = \frac{L(\epsilon_{n+1}, \dots, \epsilon_o)}{(\epsilon'_n, \dots, \epsilon'_1, \epsilon_o)} \delta_{\epsilon_n, \epsilon'_n, \dots, \epsilon_1, \epsilon'_1, \epsilon_o, \epsilon'_o} \quad (4)$$

where $L(\epsilon_n, \dots, \epsilon_o)$ is the length of an interval belonging to the tree. The Kronecker delta's ensure that the two intervals being compared have the same history in the tree construction. The sequence of ϵ 's describes the location of the intervals in the tree structure, and assume the binary values of 0 or 1. For the circle map, the sequence $(\epsilon_{i+1}, \epsilon_i) = (1, 1)$ is forbidden, consistent with the Fibonacci sequence defining the periodic orbits. The argument of the function is determined by expanding time (or iterations) in base 2, i.e., $t = \sum \epsilon_i 2^i$, yielding $\sigma(t)$. After suitable normalization, this procedure associates a real number between 0 and 1 to each interval. Such an expansion also correctly organizes the intervals to be compared. It should be stressed that if one can extract the scaling function from the experiment, one has a complete microscopic description of how the attractor was refined, and one can easily compute all statistical averages.

We shall now assume that the two entities, namely the flow and the map, possess the same multiplicative structure, leading to a particular kind of scaling at finer and finer scales. We now like to quantify the refinement process by extracting the values of scale contractions at each stage of refinement and comparing them with those from the circle map. Here one runs into the difficulty that the scaling function is experimentally not a robust quantity and therefore difficult to obtain. We therefore extract a suitably modified scaling function [17], which is based on comparing intervals within a single periodic orbit rather than two orbits. Focusing on the golden mean winding number, we note that the ratios p/q , which approximate the golden mean successively better for each increasing index on the Fibonacci sequence, correspond to the different frequency-locked Arnol'd tongues mentioned earlier. We thus need to study

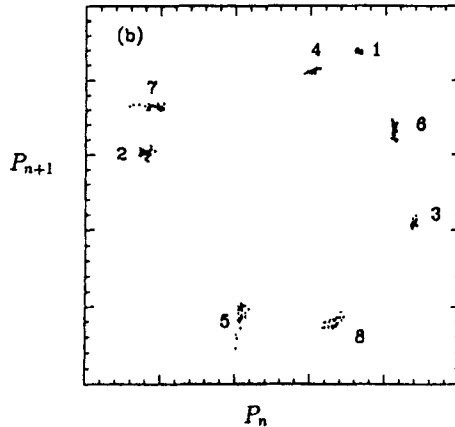


Figure 5. A typical Poincaré section for the mode-locked state for the ratio $p/q = 5/8$. The numbers by the point clusters represent the dynamical sequence of the periodic iterates creating the attractor. The sequence 1-6-3-8-5-2-7-4 is consistent with the circle map theory. The Poincaré section is embedded in three-dimensional phase space whose two-dimensional projection is presented. Three dimensional vector distances between neighboring points are used to determine the trajectory scaling function.

periodic orbits of length $F_i = q$, where $\theta_n = \theta_{n+q}$. It follows that θ_n and $\theta_{n+F_{i-1}}$ are nearest neighbors on the Poincaré section, θ_n and $\theta_{n+F_{i-2}}$ are the next nearest neighbors, and so forth. Following Ref. [17], we define the trajectory scaling function within a single periodic orbit for the circle map as

$$\sigma_j = \frac{[\theta_j - \theta_{j+F_{n-2}}]}{[\theta_j - \theta_{j+F_{n-1}}]} \quad \text{if } 0 < j \leq F_{n-2} \quad (5)$$

and

$$\sigma_j = \frac{[\theta_j - \theta_{j+F_{n-2}}]}{[\theta_j - \theta_{j-F_{n-1}}]} \quad \text{if } F_{n-2} < j \leq F_n. \quad (6)$$

Since we wish to approach the golden mean critical point with a sequence of p/q rational approximations, we experimentally adjust the system at the critical amplitude to the best possible rational approximation to the golden mean winding number. For any given p/q approximation, the Poincaré section consists of a set of q discrete points. For the experimental situation, a two-dimensional projection for $q = 8$ is shown in figure 5. The experimental trajectory scaling function is obtained using the three-dimensional vector distances between the appropriate points. The noise within each point cluster is reduced by averaging. The experimental trajectory scaling function for a $5/8$ lock-in state is shown in figure 6. The reader should examine figure 6 with figure 4 of Ref. [17] to realize that the present comparison is actually of better quality than for the convection experiment considered there. The agreement between theory and experiment is reasonably good, though more data points and smaller experimental error would have been desirable.

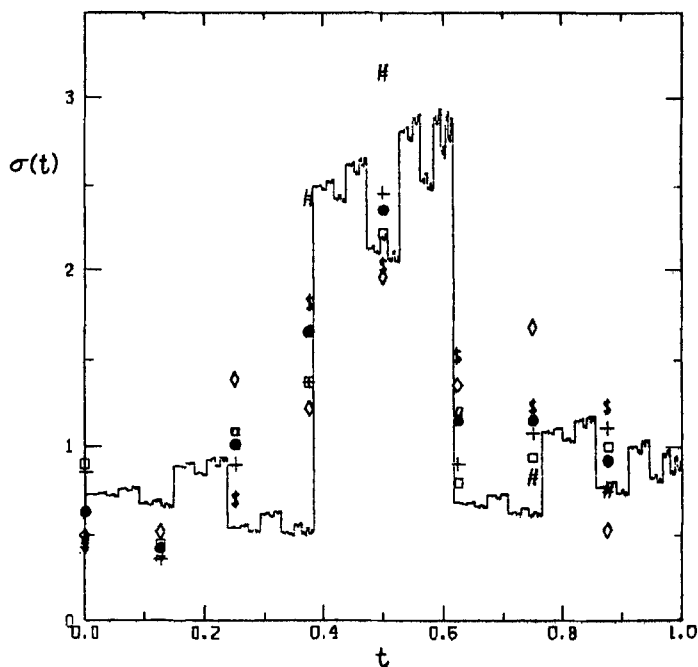


Figure 6. The trajectory scaling function from the experiment for a $5/8$ lock-in state. The solid line is computed from the sine circle map at the golden mean critical point. The various symbols represent calculations from different experimental runs.

7. Conclusions

Even though some departures from the universality associated with the circle map are apparent in wake dynamics, we think that the extent of the observed similarity is remarkable. It is not obvious whether the departures observed are real or occur because the control parameters are not as fine tuned as desired. It is known, for example, that departures from criticality can produce comparable departures from universality to those observed here [18]. Apropos of this state of affairs, we reiterate that enormous care was exercised in the experiments, and state our belief that the residual problems of fine control cannot be eliminated without resorting to unconventional ways of generating such flows. A particular focus of this work has been the search for universal behavior through the study of the trajectory scaling function. This gives a detailed description of the attractor. We believe that the agreement with universality predictions for this experimentally fragile but rich function is indeed considerable.

In the past, observations such as these have evoked the question: why does a fluid flow governed by coupled field equations follow the dynamics of a simple map? The key idea here is universality: *a system may exhibit quantitative universality as long as it possesses certain common qualitative properties*. The relevant statement here is that the dynamics of many systems with two nonlinearly coupled modes, one of which is periodically driven, yield the dynamics of a sine circle map near the critical point. It must be said that at present there are no general rules that help us forecast with certainty that a

flow in which a few modes are excited will or will not follow a certain universal scenario. However, with the hindsight of the experimental (or other) knowledge about the existence of a universal scenario, it is often possible to derive the simple map from the governing equations.

In the particular case of the oscillating cylinder, the experimental demonstration of the correspondence between the flow and the circle map implies that one should be able to extract the latter appropriately from the equations of motion governing the flow. Without this step, the connections implied are unsatisfying and, to a skeptical mind, perhaps no more than a curiosity. Some work in the needed direction has already occurred [11]. The starting point is the Landau-Stuart equation [19], [20] which, on the one hand, can be deduced from the equations of motion and, on the other hand, is also known to describe the wake evolution near the critical Reynolds number [21], [22]. Add to this equation an external forcing term $F = F_o \exp(i\omega_e t)$, in the same spirit as that of the oscillating cylinder experiment. From this one can generate a coupled dynamical system for the amplitude and phase of a disturbance in the forced wake. An analytical study of even this simplified dynamical system is too complex, but its numerical study shows features that are close to those observed. In the limit of low forcing, this dynamical system indeed reduces to the circle map.

Acknowledgements

The research was supported by grants to Yale University awarded by the Air Force Office of Scientific Research and the Defense Advanced Research Projects Agency. KRS appreciates the hospitality of the School of Mathematics, Institute for Advanced Study, Princeton, while completing this paper.

References

- [1] H Bai-Lin, *Chaos II* (World Scientific, Singapore, 1990)
- [2] M J Feigenbaum, L P Kadanoff and S J Shenker, *Physica* **D5**, 370 (182)
- [3] S J Shenker, *Physica* **D5**, 405 (1982)
- [4] S Ostlund, D Rand, J Sethna and E Siggia, *Physica* **D8**, 303 (1983)
- [5] D J Olinger and K R Sreenivasan, *Phys. Rev. Lett.* **60**, 797 (1988)
- [6] D J Olinger and K R Sreenivasan, "Universal dynamics in the wake of an oscillating cylinder at low Reynolds number," in *ASME symposium on flow induced vibrations: Nonlinear interaction effects and chaotic motions*, ASME Winter Annual Meeting, Chicago, Illinois, pp. 1-27 (1988)
- [7] J Stavans, F Heslot and A Libchaber, *Phys. Rev. Lett.* **55**, 596 (1985)
- [8] J Stavans, *Phys. Rev.* **A35**, 4314 (1987)
- [9] M J Feigenbaum, M H Jensen and I Procaccia, *Phys. Rev. Lett.* **57**, 1503 (1986)
- [10] D J Olinger, *Phys. Fluids* **5**, 1947 (1993)
- [11] D J Olinger, "Universality in the transition to chaos in open fluid flows", Ph.D. Thesis, Yale University, 1990
- [12] A Roshko, N.A.C.A. Tech. Rep. 1191, 1954
- [13] See, for example, T C Halsey, M H Jensen, L P Kadanoff, I Procaccia and B I Shraiman, *Phys. Rev.* **A33**, 1141 (1986)
Aspects of multifractals were introduced in the context of strange attractors by H G E Hentschel and I Procaccia, *Physica* **D8**, 435 (1983)

Chaos and oscillating cylinder

In the context of turbulence, they were introduced differently by G Parisi and U Frisch, in *Turbulence and predictability in geophysical fluid dynamics*, edited by M Ghil *et al*, North Holland, pp. 719–736;

Their rudiments can be found in an even earlier paper by B B Mandelbrot, *J. Fluid Mech.* **62**, 331, 1974

For a discussion of multifractals in experimental contexts, see C Meneveau and K R Sreenivasan, *J. Fluid Mech.* 429–484 (1991)

- [14] A B Chhabra, R V Jensen and K R Sreenivasan, *Phys. Rev.* **A40**, 4593 (1989)
- [15] M J Feigenbaum, *J. Stat. Phys.* **19**, 25 (1978)
- [16] M J Feigenbaum, *J. Stat. Phys.* **21**, 669 (1979)
- [17] A L Belmonte, M J Vinson, J A Glazier, G H Gunaratne and B G Kenney, *Phys. Rev. Lett.* **61**, 539 (1988)
- [18] J A Glazier, G Gunaratne and A Libchaber, *Phys. Rev.* **A37**, 523–530 (1988)
- [19] L D Landau and E M Lifshitz, *Fluid Mechanics: Course in Theoretical Physics* (Pergamon Press, Oxford, 1959) vol. 6 ch. 3
- [20] J T Stuart, *J. Fluid Mech.* **9**, 353 (1960)
- [21] C Mathis, M Provansal and L Boyer, *J. Fluid Mech.* **182**, 1 (1987)
- [22] K R Sreenivasan, P J Strykowski and D J Olinger, “Hopf bifurcation, Landau equation, and vortex shedding behind circular cylinders”, in *ASME Forum on Unsteady Flow Separation*, FED **52**, 1 (1987)